JACS
JOURNAL OF THE AMERICAN CHEMICAL SOCIETY
Communication
pubs.acs.org/JACS

Experimental and Computational Evidence for a Loose Transition State in Phosphoroimidazolide Hydrolysis

Li Li, Victor S. Lelyveld, Noam Prywes, and Jack W. Szostak*

Howard Hughes Medical Institute, Department of Molecular Biology and Center for Computational and Integrative Biology, Massachusetts General Hospital, Boston, Massachusetts 02114, United States

Supporting Information

ABSTRACT: Phosphoroimidazolides play a critical role in several enzymatic phosphoryl transfer reactions and have been studied extensively as activated monomers for nonenzymatic nucleic acid replication, but the detailed mechanisms of these phosphoryl transfer reactions remain elusive. Some aspects of the mechanism can be deduced by studying the hydrolysis reaction, a simpler system that is amenable to a thorough mechanistic treatment. Here we characterize the transition state of phosphoroimidazolide hydrolysis by kinetic isotope effect (KIE) and linear free energy relationship (LFER) measurements, and theoretical calculations. The KIE and LFER observations are best explained by calculated loose transition structures with extensive scissile bond cleavage. These three-dimensional models of the transition state provide the basis for future mechanistic investigations of phosphoroimidazolide reactions.

Phosphate esters confer a stable backbone upon nucleic acids and are ubiquitous in biochemical reactions.[1] Phosphoroimidazolides, being much more labile, have been mainly found as enzymatic intermediates, such as those formed by acid phosphatase[2] and the RtcB RNA ligase.[3] Their reactivity has been exploited in laboratory efforts to synthesize self-replicating model protocells,[4] in which nucleoside 5′-phosphoroimidazolides are used as activated substrates to chemically copy RNA templates (Scheme 1).[5] Resolving the transition structures of these phosphoryl transfer reactions will advance our understanding of enzymatic reactions and may guide optimization of nonenzymatic RNA replication,[6] potentially enabling the replication of a broader range of template sequences inside model protocells.[7]

Scheme 1. Model Systems for the Study of Nonenzymatic RNA Replication

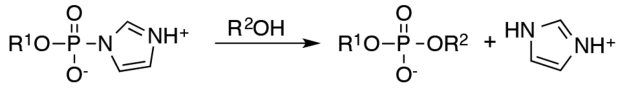

Primer extension	R^1 = Nucleoside	R^2 = Primer
Hydrolysis reaction	R^1 = Nucleoside	R^2 = H
Computational model	R^1 = Me	R^2 = H

A good model system for such a mechanistic study is the hydrolysis reaction (Scheme 1). Earlier work by Kanavarioti et al. on the hydrolysis pH–rate profile suggested that from pH 4 to 10 hydrolysis occurs via the attack of water on a phosphoroimidazolium zwitterion with a deprotonated phosphate and a protonated leaving group.[8] To obtain insight into the transition state structures, additional experimental and computational tools are necessary. These include kinetic isotope effect (KIE) and linear free energy relationships (LFER) that probe changes in bonding and charge distribution in the transition state, respectively, as well as quantum mechanical calculations that provide three-dimensional transition structures to better interpret these experimental results.

Phosphoryl transfer reactions may proceed via three mechanisms: an S_N1-like stepwise mechanism with a metaphosphate intermediate ($D_N + A_N$ per IUPAC nomenclature), a stepwise $A_N + D_N$ mechanism with a phosphorane intermediate, and an S_N2-like concerted A_ND_N mechanism in which the bond formation to the nucleophile and the bond fission to the leaving group both occur in the transition state (Figure S1).[2] The transition state of the A_ND_N mechanism is loose if it has less axial bonding than the ground state, or tight if it has more.[9] Extensive KIE and LFER studies have shown that phosphate esters hydrolyze via either the A_ND_N or $A_N + D_N$ mechanisms. Furthermore, as the alkylation state of the phosphate increases from monoesters to triesters, the transition state tightens with less scissile bond fission.[2,9,10]

To characterize the extent of scissile bond fission in the transition state of phosphoroimidazolium hydrolysis, we determined the leaving-group KIE by hydrolyzing guanosine-5′-phosphoroimidazolide (ImpG) **1a** and its ^{15}N-labeled isotopologue **1b** (Figure 1) at pH 4.0 using the competitive method by mass spectrometry (Figure S2).[11,12] The observed KIE for the hydrolysis of **1a** relative to **1b**, ^{15}k, was 1.019 ± 0.002 from eight independent measurements (Figure 1). Its large amplitude suggests that the hydrolytic rate-limiting step involves extensive scissile bond fission, indicating an A_ND_N mechanism with a loose transition state (Supporting Text 1).

We next measured the KIE for hydrolysis of phosphoroimidazolides **1a** relative to **1c**, or ^{18}k. The observed KIE is 1.002 ± 0.003 (Figure 1). Since the ^{18}O isotope effect for phosphate protonation is inverse, between 0.98 and 0.99,[13,14] the observed KIE is consistent with the phosphate remaining deprotonated at the rate-limiting step (Supporting Text 2).

Received: January 22, 2016
Published: March 14, 2016

DOI: 10.1021/jacs.6b00784
J. Am. Chem. Soc. 2016, 138, 3986–3989

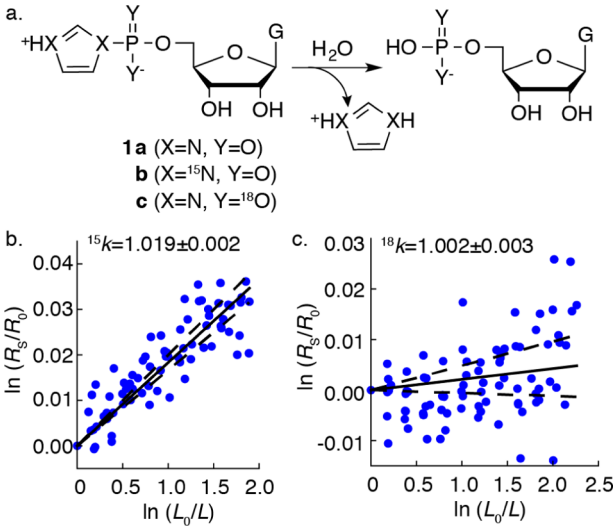

Figure 1. Isotopologues and their kinetic isotope effects. (a) The reaction scheme for hydrolysis of isotopologues. (b) KIE measurement for **1a** vs **1b**. (c) KIE measurement for **1a** vs **1c**. The KIE was determined by measuring R_S, the enrichment of the heavy to light isotopologues of the substrate ImpG, over the reaction course. R_S is normalized by the initial ratio R_0. L is the integrated intensity of the light isotopologue, and it is normalized by the initial intensity L_0. The solid and dashed lines in (b) and (c) are fits using KIEs of the mean and the limits of 95% confidence interval (n = 8).

To obtain structural insight into the transition state, we complemented these KIE measurements with quantum mechanical calculations. The validity of these computational models was judged by comparing the theoretical KIEs calculated using the Bigeleisen–Mayer equation[15] with the experimental results. Although this powerful approach has repeatedly provided critical transition-structure insights of important reactions,[16−18] its application in phosphoryl transfer reactions is limited[19,20] due to the difficulties in modeling the strong phosphate-solvent interactions.[21] Recent advances[20,21] overcome this technical difficulty by the microsolvation approach, in which an explicit model of the solute and a few key solvent molecules is embedded in an implicit solvent model. This method calculates isotope effects to high accuracy at an affordable computational cost.[20,21]

Our computational model of the hydrolysis reaction retains all the key elements of phosphoroimidazolium hydrolysis (Scheme 1). Using the microsolvation approach, we built a series of models with up to eight explicit water molecules that occupied most hydrogen-bonding sites of the reactants. These microsolvated structures provide a more comprehensive and accurate sampling of the experimental transition-state ensemble, which includes various transition structures with different solvation shells. The structures were optimized at the B3LYP/6-31+G(d)/PCM level of theory,[22−24] which has been successful in elucidating mechanisms of phosphate ester hydrolysis.[19,25,26] Additional calculations performed at different levels of theory confirmed the nature of the stationary points and yielded similar geometries (Figures S3 and S4) and calculated KIEs (Table S1), suggesting that the results are independent of the theoretical level. All calculated transition structures belong to the A_ND_N mechanism (Scheme 2). We further classified these transition structures into a loose A_ND_N (sum of axial bond order less than 1, Table S2) and a tight A_ND_N mechanism (sum of axial bond order greater than 1, Table S3).[9]

Scheme 2. Summary of Calculated A_ND_N Mechanisms; Calculated P−N Bond Lengths Are Labeled in Å

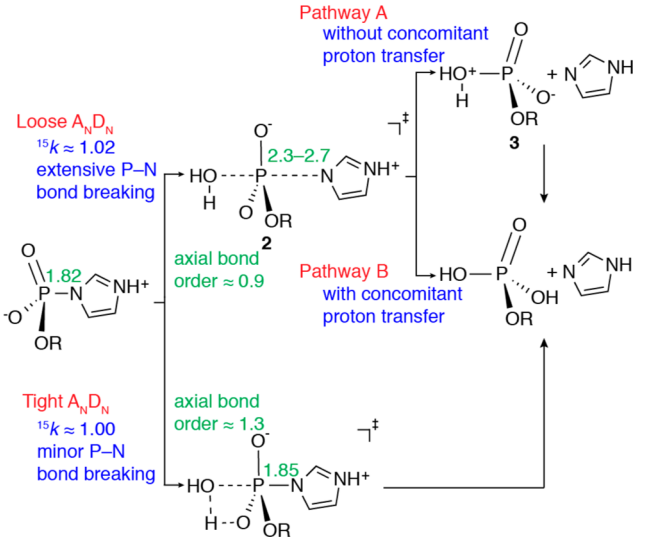

In the loose A_ND_N mechanism, the hydrolysis proceeds via a rate-determining transition structure (**2**, Figure 2) with

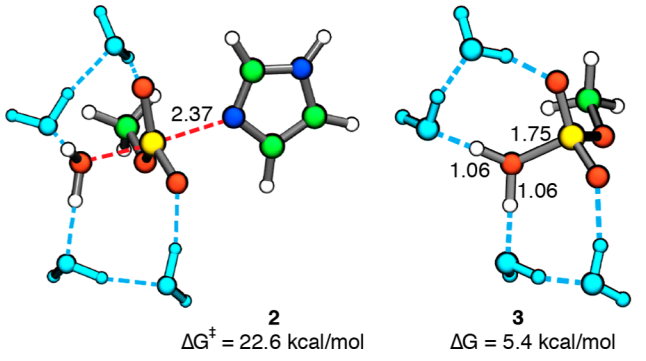

Figure 2. Representative transition structure **2** and intermediate **3** of the loose A_ND_N mechanism. Key distances are labeled in Å. Gibbs free energies are relative to reactants. In the intermediate, the leaving group is separated infinitely from **3**. Water molecules, except for the nucleophile, are shown in cyan.

extensive scissile bond fission. In contrast to the planar metaphosphate-like phosphoryl group in the *p*-nitrophenol phosphate (*p*NPP) dianion,[20] the phosphoryl group in **2** deviates from a planar structure by ∼10° (Figure S3 and Table S2). Depending on the local solvent structure, **2** can lead to a hydrolyzed product either via a concomitant proton transfer (Scheme 2, Pathway B), or via a zwitterionic intermediate (**3**, Figure 2, and Scheme 2, Pathway A). The oxonium ion **3** has elongated O−P and O−H bonds, and a structurally similar intermediate has been reported in *p*NPP dianion hydrolysis.[20] Figures S5 and S6 show representative intrinsic reaction coordinates for both pathways of the loose mechanism. In the following discussion, we consider these two pathways collectively because their rate-limiting transition structures are similar (Table S2) and **3** is expected to be short-lived due to its low pK_a (ca. −4).[27]

A close inspection of various microsolvated transition structures (Figures S7 and S8) revealed that additional explicit

DOI: 10.1021/jacs.6b00784
J. Am. Chem. Soc. 2016, 138, 3986−3989

solvent molecules stabilized **2** (Table S4) and shortened its P−N bond distance (Table S2). The energies and geometries showed significant variation as the number of explicit solvent molecules increased from one to three, but seemed to converge with more than three solvent molecules. Importantly, the calculated ^{15}k and ^{18}k from these transition structures both agreed well with the experimental measurement (Tables 1 and S5).

Table 1. Experimental and Calculated KIEs of ImpG Hydrolysis

	loose (Pathway A)		tight	
no. of H_2O[a]	^{15}k	^{18}k	^{15}k	^{18}k
0			0.999	0.995
1	1.027	1.001	0.999	1.001
2	1.025	1.002	0.999	1.000
3	1.021	1.002	0.999	1.002
4	1.021	1.002	0.999	0.999
5	1.021	1.002	1.000	0.999
6	1.021	1.002	1.000	0.998
7	1.022	1.001	0.999	0.999
8	1.023	1.001	0.999	0.997

	^{15}k	^{18}k
observed[b]	1.019(2)	1.002(3)

[a]Number of solvent molecules in the calculation except for the nucleophile. [b]Limits of the 95% confidence interval in the last digit (n = 8) are shown in parentheses.

The transition structures of the tight A_ND_N mechanism have a distorted trigonal bipyramidal phosphorus center (Figures S4 and S9) and they show little scissile bond fission (Table S3) with predicted ^{15}k close to 1 (Table 1). Transition structures obtained by progressive microsolvation (Figure S9) showed little geometric (Figure S10 and Table S3) and energetic variation (Table S6). All calculated reaction barriers of the tight mechanism were much higher than those of the loose mechanism (Figure S11) as well as the experimental activation energy (Figure S12). Critically, although the calculated ^{18}k for the tight mechanism fell in the range of the experimental results, the calculated ^{15}k did not (Table 1). These results disfavor the tight A_ND_N mechanism.

The extensive calculated P−N bond fission predicts that leaving group ability should have a strong influence on the hydrolysis rate. A linear correlation between the leaving group pK_a and the logarithm of the hydrolysis rate was found with a series of phosphoroimidazolides (Figures 3 and S13). The large negative slope (Brønsted value, or β_{lg}) of −1.49 supports the loose A_ND_N mechanism, and is comparable to the values of −1.23 of *p*NPP dianions[27] and −1.1 of phosphorylated pyridines.[28] Interestingly, although 2-MeImpG hydrolyzes 21-fold more slowly than **1a**, it condenses about 10-fold faster in nonenzymatic primer extension.[29] The precise role of the 2-methyl group in stimulating primer extension is still unclear, and will be an important focus of future studies.

In conclusion, our quantum mechanical calculations provide a three-dimensional transition-state model that unifies the experimental KIEs and β_{lg} of phosphoroimidazolide hydrolysis. At the transition state, there is significant P−N bond fission without forming a metaphosphate-like phosphoryl group. This is distinct from the much tighter transition state of phosphate diesters[19] as well as the loose yet metaphosphate-like transition state of the *p*NPP dianion.[20] This difference is likely due to the weaker P−N bond, a fundamental difference between phosphoroimidazolides and phosphate esters.

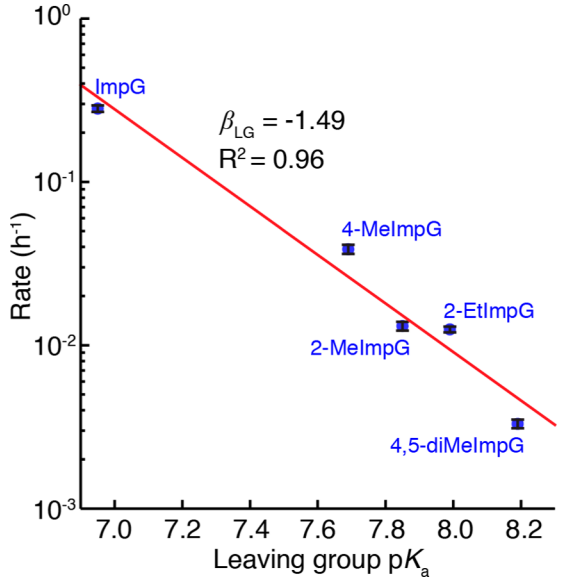

Figure 3. Dependence of the hydrolysis rates on the leaving group pK_a for phosphoroimidazolides. The red line is the least-squares fit to the data. Error bars show one standard deviation (n = 5).

■ ASSOCIATED CONTENT

Supporting Information

The Supporting Information is available free of charge on the ACS Publications website at DOI: 10.1021/jacs.6b00784.

Materials and methods, supporting text, Figures S1−S13, Tables S1−S7, and energies and full geometries of all calculated structures (PDF)

■ AUTHOR INFORMATION

Corresponding Author

*szostak@molbio.mgh.harvard.edu

Notes

The authors declare no competing financial interest.

■ ACKNOWLEDGMENTS

J.W.S. is an Investigator of the Howard Hughes Medical Institute. L.L. is a Life Sciences Research Foundation Fellow. This work was supported in part by a grant (290363) from the Simons Foundation to J.W.S. The authors thank Szostak lab members Dr. A. C. Fahrenbach, Dr. N. P. Kamat, Dr. A. Pal, J. Tam, and T. Walton for assistance with the synthesis and Dr. Eugene Kwan (Harvard University) for helpful discussions. Computations were run on the Odyssey cluster supported by the FAS Division of Science, Research Computing Group, at Harvard University.

■ REFERENCES

(1) Westheimer, F. H. *Science* **1987**, *235*, 1173.
(2) Cleland, W. W.; Hengge, A. C. *Chem. Rev.* **2006**, *106*, 3252.
(3) Chakravarty, A. K.; Subbotin, R.; Chait, B. T.; Shuman, S. *Proc. Natl. Acad. Sci. U. S. A.* **2012**, *109*, 6072.
(4) Blain, J. C.; Szostak, J. W. *Annu. Rev. Biochem.* **2014**, *83*, 615.
(5) Inoue, T.; Orgel, L. E. *J. Am. Chem. Soc.* **1981**, *103*, 7666.

DOI: 10.1021/jacs.6b00784
J. Am. Chem. Soc. 2016, 138, 3986−3989

(6) Szostak, J. W. *J. Syst. Chem.* **2012**, *3*, 2.
(7) Adamala, K.; Szostak, J. W. *Science* **2013**, *342*, 1098.
(8) Kanavarioti, A.; Bernasconi, C. F.; Doodokyan, D. L.; Alberas, D. J. *J. Am. Chem. Soc.* **1989**, *111*, 7247.
(9) Lassila, J. K.; Zalatan, J. G.; Herschlag, D. *Annu. Rev. Biochem.* **2011**, *80*, 669.
(10) Hengge, A. C. *Acc. Chem. Res.* **2002**, *35*, 105.
(11) Berti, P. J.; Blanke, S. R.; Schramm, V. L. *J. Am. Chem. Soc.* **1997**, *119*, 12079.
(12) Harris, M. E.; Dai, Q.; Gu, H.; Kellerman, D. L.; Piccirilli, J. A.; Anderson, V. E. *J. Am. Chem. Soc.* **2010**, *132*, 11613.
(13) Knight, W. B.; Weiss, P. M.; Cleland, W. W. *J. Am. Chem. Soc.* **1986**, *108*, 2759.
(14) Hengge, A. C.; Edens, W. A.; Elsing, H. *J. Am. Chem. Soc.* **1994**, *116*, 5045.
(15) Bigeleisen, J.; Mayer, M. G. *J. Chem. Phys.* **1947**, *15*, 261.
(16) Houk, K. N.; Gustafson, S. M.; Black, A. K. *J. Am. Chem. Soc.* **1992**, *114*, 8565.
(17) Storer, J. W.; Raimondi, L.; Houk, K. N. *J. Am. Chem. Soc.* **1994**, *116*, 9675.
(18) Ussing, B. R.; Singleton, D. A. *J. Am. Chem. Soc.* **2005**, *127*, 2888.
(19) Wong, K.-Y.; Gu, H.; Zhang, S.; Piccirilli, J. A.; Harris, M. E.; York, D. M. *Angew. Chem., Int. Ed.* **2012**, *51*, 647.
(20) Duarte, F.; Åqvist, J.; Williams, N. H.; Kamerlin, S. C. *J. Am. Chem. Soc.* **2015**, *137*, 1081.
(21) Kolmodin, K.; Luzhkov, V. B.; Åqvist, J. *J. Am. Chem. Soc.* **2002**, *124*, 10130.
(22) Becke, A. D. *J. Chem. Phys.* **1993**, *98*, 5648.
(23) Lee, C.; Yang, W.; Parr, R. G. *Phys. Rev. B: Condens. Matter Mater. Phys.* **1988**, *37*, 785.
(24) Tomasi, J.; Mennucci, B.; Cammi, R. *Chem. Rev.* **2005**, *105*, 2999.
(25) Ribeiro, A. J. M.; Ramos, M. J.; Fernandes, P. A. *J. Chem. Theory Comput.* **2010**, *6*, 2281.
(26) Lopez, X.; Schaefer, M.; Dejaegere, A.; Karplus, M. *J. Am. Chem. Soc.* **2002**, *124*, 5010.
(27) Kirby, A. J.; Varvoglis, A. G. *J. Am. Chem. Soc.* **1967**, *89*, 415.
(28) Jameson, G. W.; Lawlor, J. M. *J. Chem. Soc. B* **1970**, 53.
(29) Wu, T.; Orgel, L. E. *J. Am. Chem. Soc.* **1992**, *114*, 5496.

DOI: 10.1021/jacs.6b00784
J. Am. Chem. Soc. 2016, 138, 3986−3989